

## “AN OPTIMUM PERFORMANCE OF A FLAT - TYPE SOLAR AIR HEATER WITH A POROUS ABSORBER”

By

**M.A. Hassab,**

Mechanical Engineering Dept.,  
Faculty of Engineering,  
Qatar University, Doha,  
Qatar, Arabian Gulf.

**M.M. Sorour and F.A. Elewa,**

Mechanical Engineeringf Dept.,  
Alexandria University,  
Alexandria, Egypt.

### ABSTRACT

This investigation is concerned with the design and performance of a flat solar air heater in which air flows perpendicular from a vented transparent cover through a porous absorber plate. The design phase involves a stability analysis to determine the critical distance (maximum allowable distance) between the absorber and transparent plates, for suppressing convection currents, under a variety of environmental and operating conditions. These results are expected to be useful to designers of solar collectors.

In addition, the thermal performance of this solar heater at its optimum design conditions was computed for a wide range of system parameters illustrating the contributions of conduction and radiative modes of heat transfer. The results indicate that best operating efficiency can be obtained when running the collector with mass flow rate,  $m > 40 \text{ Kg/m}^2 \text{ hr}$ .

### 1. INTRODUCTION

Solar collectors are known to be inherently unstable to the natural convection currents which occur as a result of the temperature difference between the absorber plate and the transparent glass cover. The natural convection losses represent 30–40% of the total heat losses in solar collectors which comprise

nearly 50% of the total solar energy received at the cover surface under normal operating conditions. Consequently, smaller collector areas can be used or higher temperatures may be obtained when convection losses are prohibited or reduced.

The most common method employed to reduce natural convective currents is by placing a vertical cellular structure with highly reflecting walls absorbing infrared radiation, known as a honeycomb, between the absorber plate and the transparent cover. These devices have different geometric configurations, and have been used by various investigators to increase the shear surfaces within the fluid layer [1–3]. It has been shown theoretically [4–5] and confirmed experimentally [6] that the honeycomb structures raise the critical Rayleigh number which characterizes the onset of convection in a horizontal fluid layer heated from below.

For an inclined air layer, which is the case for solar air heaters and for Rayleigh numbers greater than the critical value, the use of honeycomb devices for convection suppression is of little importance [2]. In addition, the thermal efficiency is negatively influenced by the thickness and physical properties of the honeycomb walls since both conduction losses and solar transmittance depend on these factors. Therefore, although honeycomb devices are very effective under some conditions, their commercial use is questionable due to their high manufacturing cost.

This investigation deals with a new concept of solar air heater design where the total air flows perpendicular through a vented transparent cover to the porous absorber plate without additional components, or honeycomb structures to the assembly. In addition, the air heater is designed such that no natural convective currents take place under various system parameters.

## 2. ANALYSIS

The physical model is composed of an upper transparent cover, a lower black porous plate, insulating material and an air supply mechanism as indicated in Figure 1. The analytical study of this model leading to its optimal design requires that a stability analysis be made of the fluid motion. This part determines the conditions at which natural convection currents can be prevented. A review of literature reveals that the published work on this problem is only limited for the horizontal position with a small range of wall Reynolds numbers [7 & 8].

Therefore, these published works are not sufficient for the analysis of the proposed solar collector under its normal operating conditions. As a result, the previous analysis is extended for a wide range of wall Reynolds numbers with the consideration of the inclination of the collector.

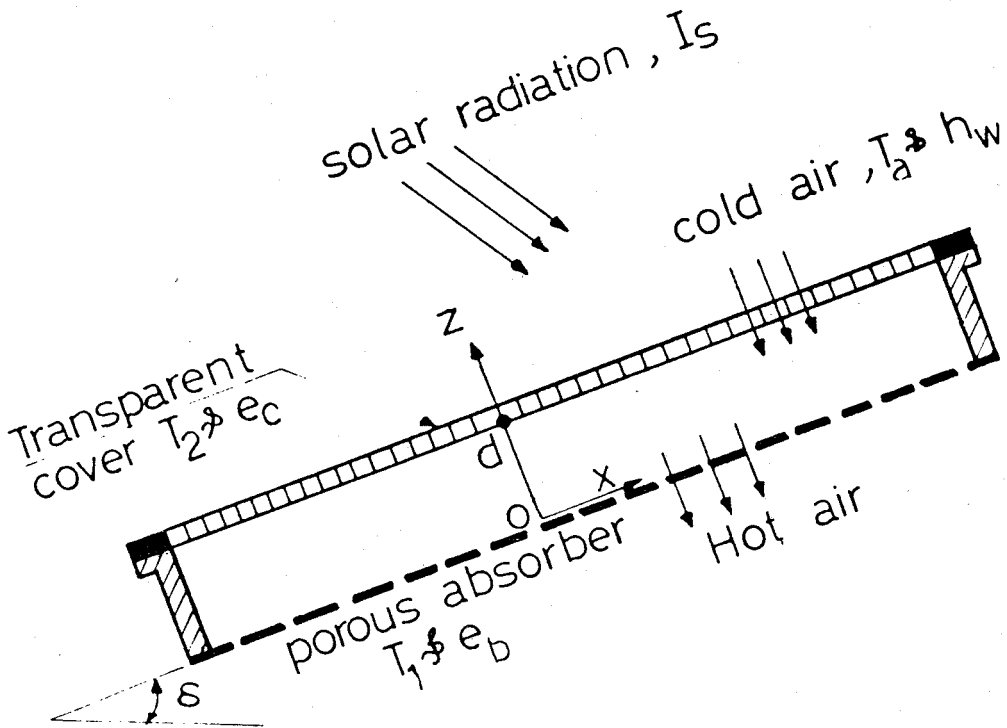


Fig. (1) : Schematic Diagram of Air Heater.

As a normal procedure, small quantities of velocity, pressure, density and temperature are introduced to the uniform motion of the air.

$$u = \bar{u} + u' \quad , \quad v = \bar{v} + v' \quad , \quad w = \bar{w}_o + w' \quad , \quad p = \bar{p} + p' \quad (1)$$

$$T = \bar{T} + T' \quad , \quad \rho = \bar{\rho} + \rho'$$

*An Optimum Performance of a Flat-typed Solar Air Heater*

where the bar refers to mean quantities and the primes denote the small perturbations. Introducing these variables into the conservation equations of mass, momentum and energy, using the Boussinesq approximation, and neglecting nonlinear terms, the resulting equations governing the formation of the longitudinal disturbances, which are dominant up to collector inclination angles less than 45°,  $\delta \leq 45$  [9], are given in dimensionless form as:

$$\frac{\partial \hat{V}}{\partial Y} + \frac{\partial \hat{W}}{\partial Z} = 0 \quad (2)$$

$$\left( \frac{\partial}{\partial t} - \nabla^2 \right) \hat{V} - Re \frac{\partial \hat{V}}{\partial Z} = - \frac{\partial \hat{P}}{\partial Y} \quad (3)$$

$$\left( \frac{\partial}{\partial t} - \nabla^2 \right) \hat{W} - Re \frac{\partial \hat{W}}{\partial Z} = - \frac{\partial \hat{P}}{\partial Z} + (Ra \cdot \cos \delta) \hat{\theta} \quad (4)$$

$$\left( Pr \frac{\partial}{\partial t} - \nabla^2 \right) \hat{\theta} - Pe \frac{\partial \hat{\theta}}{\partial Z} + D \hat{\theta} \hat{W} = 0 \quad (5)$$

Subject to the following boundary conditions at the absorber and cover:

$$\hat{V} = \hat{W} = \hat{\theta} = 0 \quad \text{at} \quad Z = 0, 1 \quad (6)$$

Here,  $\nabla^2 = \frac{\partial^2}{\partial Y^2} + \frac{\partial^2}{\partial Z^2}$  Pr, Pe, Re and Ra are the Prandtl number,

Peclet number (Pe = Pr · Re), Reynolds number and Rayleigh number respectively,  $\hat{V}$  and  $\hat{W}$  are perturbed velocity components in the Y and Z directions with the Y-coordinate normal to elevations plane and Z-coordinate normal to the absorber plane.  $\hat{\theta}$  is the perturbed temperature and  $\hat{P}$  is the perturbed pressure.

It should be noted that longitudinal waves governing the initiation of convection are two-dimensional and rotating symmetrically around the X-axis. For this reason, the derivatives,  $\partial^n / \partial X^n = 0$ . In addition, the fluctuations of the wall temperatures have been neglected since their thermal resistances are very small compared to the thermal resistance of the flowing air. Furthermore, the properties of the air are based on the mean temperatures of the boundaries.

The formal solution of the linear stability Equations (2-6) can be constructed in the form:

$$\hat{F}(Y, Z, t) = F(Z) e^{+ ia(Y+ct)} \quad (7)$$

Where  $\hat{F} = \hat{P}, \hat{V}, \hat{W}$  or  $\hat{\theta}$ ;  $a$  = wave number in the Y-direction;  $c = c_r + c_i$  is a complex quantity, with  $c_r$  = wave speed or the velocity of propagation of the wave in the Y-direction.  $c_i$  determines the degree of damping when  $c_i > 0$ . When the wave is growing  $c_i < 0$ .  $F^+$  is the amplitude function of the single oscillation of the disturbances function  $F$ .

The solution (7) is introduced into Equations (2-6) and when the variables  $P$  and  $V$  are eliminated among these resulting expressions; we obtain the following perturbation equations:

$$[C - (D^2 - \text{Re}D - a^2)] (D^2 - a^2) W^+ = - a^2 \text{Ra} \cdot \cos\delta \theta^+ \quad (8)$$

$$[P_r C - (D^2 - \text{Pe}D - a^2)] \theta^+ + D \bar{\theta} W^+ = 0 \quad (9)$$

$$W^+ = DW^+ = \theta^+ = 0 \quad \text{at } Z = 0, 1 \quad (10)$$

where,  $c = i \partial c$ ,  $D^n = d^n / Z^n$

The quantity  $D \bar{\theta}$  appearing in Equation (9) refers to the dimensionless base flow temperature gradient that is to be determined from the base flow analysis.

**Base-Flow Problem:**

The equation of energy governing the initial motion of the air caused by the uniform cross-flow velocity  $W_o$  through the spacing between the wall is given as:

$$\frac{d^2 \bar{T}}{dz^2} + \frac{W_o}{\alpha} \frac{d\bar{T}}{dz} = 0 \quad (11)$$

with the boundary conditions at the absorber and cover taken respectively as:

at absorber surface	at cover surface
$T = T_b, \quad Z = 0,$	$T = T_c, \quad Z = d$

(12)

The temperatures  $T_b$  and  $T_c$  are not known apriori but can be determined by taking an energy balance at each surface, where under realistic operating conditions, they are given as:

$$-k \frac{dT_b}{dz} + \frac{\bar{\sigma} (T_b^4 - T_c^4)}{\frac{1}{e_b} + \frac{1}{e_c} - 1} = I_p \quad Z = 0 \quad (13)$$

$$-k \frac{dT_c}{dz} + \frac{\bar{\sigma} (T_b^4 - T_c^4)}{\frac{1}{e_b} + \frac{1}{e_c} - 1} + I_c = h_w (T_c - T_a)$$

$$+ e_s \bar{\sigma} (T_c^4 - T_s^4) + m C_p (T_c - T_a) \quad Z = d \quad (14)$$

In Equation (14), the temperature rise of the on flowing air to the cover is considered equal to the temperature difference ( $T_c - T_a$ ) imposed on the thermal boundary layer by the wind. Here,  $\dot{m}$  is the mass flow rate/unit surface area;  $k$  and  $C_p$  are the thermal conductivity and specific heat of the air respectively.  $I_p$  and  $I_c$  are the solar radiative heat fluxes absorbed by the absorber and cover respectively.  $T_a$  and  $T_s$  are the ambient and sky temperatures respectively. They are related to each other, as given in reference [9], by the following relations:

$$T_s = T_a [0.55 + 0.207 P_w^{1/2}]^{1/4} \text{ } ^\circ\text{K} \quad (15)$$

where,  $P_w$  = partial pressure of water in the atmosphere, in cm. Hg.

In reference [10], the wind-related convection coefficient  $h_w$  is given in terms of the wind speed  $V_w$  (m/s.) by:

$$h_w = 5.7 + 5.8 V_w \text{ W/m}^2 \text{ } ^\circ\text{C} \quad (16)$$

The surface emissivities,  $e_b$ ,  $e_c$  and  $e_s$  are respectively for the porous absorber, the cover and the sky.  $\sigma$  is the Stefan-Boltzmann constant =  $5.669 \times 10^{-8} \text{ W/m}^2 \cdot \text{K}^4$ . The solution of Equation (11) under conditions (12) leads to the determination of  $D \bar{\theta}$  as:

$$D \bar{\theta} = \frac{-P_e e^{-Pe Z}}{(1 - e^{-Pe})} \quad (17)$$

The system of Equations (8–10) together with Equation (17) constitutes an eigenvalue problem. The solution of which establishes the stability criteria of the flow field.

The Galerkin method is used to solve the above system of equations by assuming trial functions for both velocity,  $W^+$  and temperature  $\theta^+$ , in the form of infinite series as:

$$W^+(Z) = \sum_{m=1}^{\infty} A_m W_m(Z) \quad (18)$$

An Optimum Performance of a Flat-typed Solar Air Heater

$$\theta^+(Z) = \sum_{m=1}^{\infty} B_m \theta_m(Z) \quad (19)$$

where, the coefficients,  $A_m$  and  $B_m$  are unknown constants. In accordance with Reference [8], the orthogonal functions,  $W_m$  and  $\theta_m$  are satisfying the boundary conditions for  $W^+$  and  $\theta^+$  respectively, and properly taken as:

$$W_m = \frac{\cosh S_m Z - \cos S_m Z}{\cosh S_m - \cos S_m} - \frac{\sinh S_m Z - \sin S_m Z}{\sinh S_m - \sin S_m}$$

$$\theta_m = \sin(m \pi z), \quad m = 1, 2, 3 \quad (20)$$

The auxiliary eigenvalues  $S_m$  are the positives of:

$$\cosh S \cdot \cos S = 1 \quad (21)$$

and the orthogonality conditions for  $W_m$  functions are respectively given as:

$$\int_0^1 W_m(Z) W_n(Z) dZ = N_m \delta_{mn}$$

$$\int_0^1 \theta_m(Z) \theta_n(Z) dZ = \frac{1}{2} \delta_{mn}$$

$$1 \quad m = n \quad (22)$$

where,  $\delta_{mn} = \begin{cases} 1 & m = n \\ 0 & m \neq n \end{cases}$

$$N_m = [\tanh S_m \cdot \sinh S_m]^{-2}$$

Having constructed solutions for  $W^+$  and  $\theta^+$  as given above, they are introduced into Equations (8 & 9), and the orthogonality condition for each of the resulting two equations is utilized. The end result leads to the following algebraic equation written in matrix form as:

$$(CH - M) \vec{X} = 0 \quad (23)$$



where, the vector  $\vec{X}$  consists of the coefficients of the series (18) and (19) and where H and M turn out to be real coefficient matrices resulting from orthogonalization. The stability of the above system is determined by the eigenvalues of the matrix,  $H^{-1}M$ . The convergence of the constructed solution is examined for a wide range of Reynolds number. It is found that the number of terms needed for an error less than 0.1% varies from 4 to 12 as Re increases from 0 up to 40. The stability results expressed by the critical Rayleigh number,  $Ra_c$  as a function of the Reynolds number, Re are presented graphically in Figure 2. As expected, suction has a very significant stabilizing effect due to its cooling effect. That is, as Re increases, the degree of stability is increased,

For the purpose of this analysis, the data of the neutral stability, at any tilt angle  $\delta < 45^\circ$  are fitted by two polynomials to cover the considered range of the Reynolds number, Re. These expressions are correlated as follows:

$$Ra_H = 1707 + 2.54 Re + 50.36 Re^2 - 0.76 Re^3 + 0.471 Re^4$$

for  $Re < 10$  (24.a)

$$Ra_H = 22250 + 3664 Re + 203.083 Re^2 + 4.166 Re^3 + 0.0566 Re^4$$

for  $10 \leq Re \leq 40$  (24.b)

where,  $Ra_H$  = Rayleigh number at horizontal position which is related to that at any angle  $\delta$  by

$$Ra = Ra_H / \cos(\delta)$$

The temperature distribution of the air through the spacing between the absorber and cover is obtained from the solution of Equation (11) given as:

$$\bar{T} = A + B e^{-Pe Z} \quad (25)$$

These stability correlations (24) are utilized simultaneously with the heat transfer analysis for the nonconvecting (base flow) system, defined by Equations (11) and (13-14), to evaluate the thermal performance of the collector.

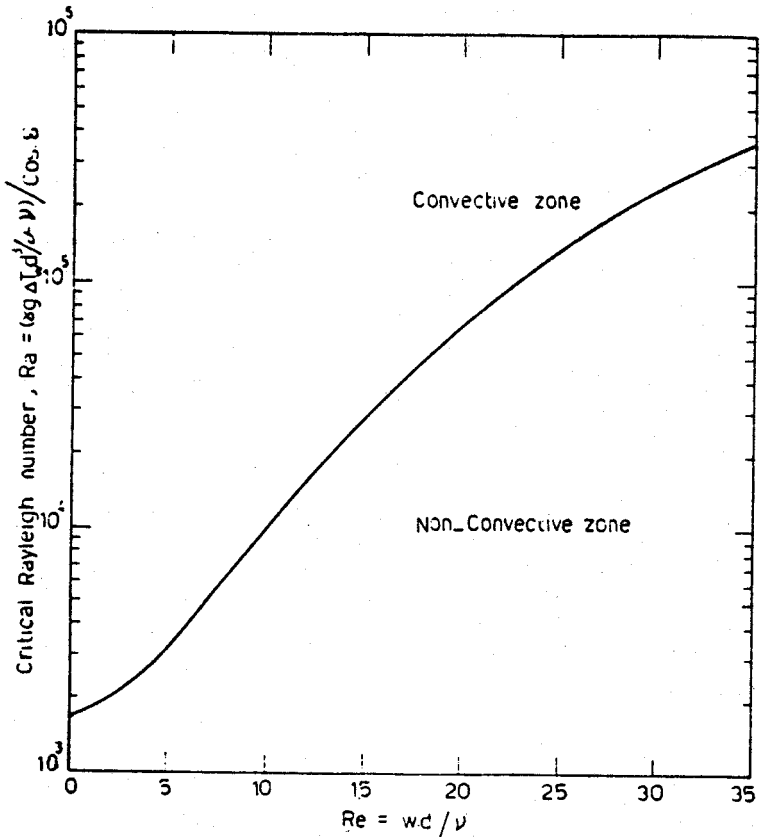


Fig. (2) : Critical Rayleigh number  $Ra$  versus wall Reynolds number  $Re$ .

### 3. THERMAL PERFORMANCE OF THE COLLECTOR:

At this stage, the thermal behaviour of the proposed collector expressed by the air temperature rise,  $\Delta T$  and the thermal efficiency is calculated under wide variations of environmental and operating conditions for the condition where stability of the fluid is satisfied.

Substituting this equation into Equations (13–14), the end results lead to two coupled equations for the coefficients, A and B. These two unknowns are also functions of a third unknown, namely, the thickness of the air layer, d. The third equation needed to solve these three unknowns is only the stability correlation (2). The critical Rayleigh number, Ra and the Reynolds number, Re defined in Equation (24) is related to these unknowns as:

$$Ra_H = \frac{g \gamma (T_b - T_c) d^3}{\alpha \nu} = \frac{g \gamma (1 - e^{-Pe}) d^3}{\alpha \nu} \cdot B$$

$$Re = \frac{md}{\rho \nu} \quad (26)$$

For stability to be achieved, the actual Rayleigh number of the system must be less than or equal to the critical one given in Equation (24). That is.

$$R_{a \text{ system}} < R_{a \text{ critical}} \quad (27)$$

Based on this concept, Equations (24) with the expression resulting from Equations (13–14) are solved numerically using the modified Newton-Raphson method to calculate the unknowns,  $T_b$ ,  $T_c$  and the thickness, d at different operating and environmental conditions.

It is to be noted that, the Rayleigh number, Ra is strongly dependent on the thickness, d as shown in Equation (26). On one hand, if d is chosen larger than the calculated (maximum) value, the critical Rayleigh number will be smaller than the system Rayleigh number, convection will ordinarily occur and the previous analysis will not be valid. On the other hand, if the value of d is taken smaller than the maximum value, the conduction and radiation losses will increase although natural convection is prevented. However, the increase in heat loss by conduction and radiation is expected to be much less than that by convection. Therefore, it is preferred to choose the value of d equal to or slightly less than its maximum value, for a specific set of operating and environmental conditions.

## An Optimum Performance of a Flat-typed Solar Air Heater

Now the efficiency, of the collector which is defined as:

$$\eta = \frac{\dot{m} c_p \Delta T}{I_s} \quad (28)$$

can be calculated at different operating and environmental conditions under provision (27).

### 4. SOLAR AIR HEATER THERMAL PERFORMANCE:

To investigate the effect of changes in operating and environmental conditions on the optimal design of the collector and its corresponding thermal performance under the provision that  $Ra \leq Ra_{critical}$ , the base case conditions were taken as follows:

1. Ambient temperature equal to the inlet air temperature,  $T_a = 25^\circ\text{C}$ .
2. Transparent cover emissivity  $e_c = 0.88$ .
3. Transparent cover emissivity  $e_{sky} = 0.87$ .
4. Collector tilt angle =  $30^\circ$ .
5. Wind speed  $V_w = 2\text{m/s}$ .
6. Porous absorber emissivity  $e_p = 0.89$  and  $0.20$ .

The effect of changes in the mass flow rate  $\dot{m}$ , the solar energy absorbed  $I_p$ , the surface emissivity of the porous absorber  $e_p$  and the wind speed  $V_w$  on the optimal air layer thickness  $d$ , are presented in Figure 3. It can be seen that for  $\dot{m} < 35 \text{ Kg/m}^2 \text{ hr}$ , the maximum thickness of the air layer becomes infinity. For this case, the critical Rayleigh number is much larger than the actual Rayleigh number of the collector.

In addition, increasing the amount of radiation reaching the absorber, decreases the maximum air layer thickness especially for higher air flow rates as illustrated in the figure. Furthermore, in comparing the effect of wall emissivity has a damping effect on the onset of convection such that a larger air layer thickness is obtained under similar conditions. However, this effect is only visible for higher flow rates and strong radiation. Lastly, the changes in wind speed was found to have a negligible effect on the optimal air layer thickness.

The variation of the air temperature rise with the various system parameters are presented in Figure 4. It can be seen that the air temperature rise is nearly proportional to the radiation intensity  $I_p$ , and inversely proportional to the emissivity  $e_p$  such that as  $e_p$  decreases, the air temperature rise significantly increases. In addition, the increase of wind speed causes a decrease in the temperature rise of air flow. However this variation decreases as the mass rate of flow increases.

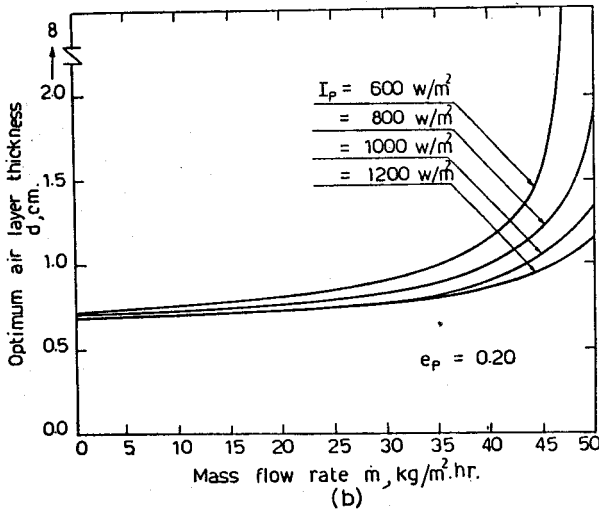
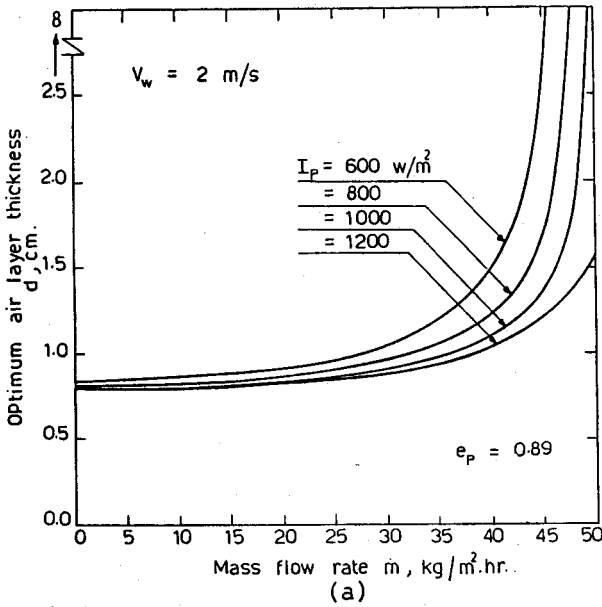


Fig. (3.a) : Mass flow rate  $m$ ,  $\text{kg/m}^2\cdot\text{hr}$ .

Fig. (3.b) : variation of the optimum air layer thickness  $d$  with the mass flow rate  $m$ , for different solar heat - fluxes  $I_p$  reaching the absorber at : a)  $e_p = 0.89$  b)  $e_p = 0.20$ .

An Optimum Performance of a Flat-typed Solar Air Heater

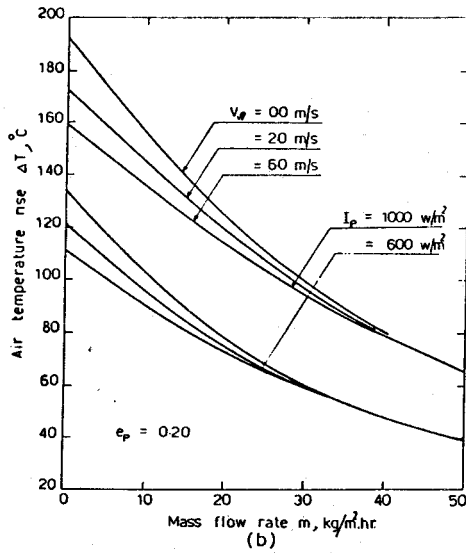
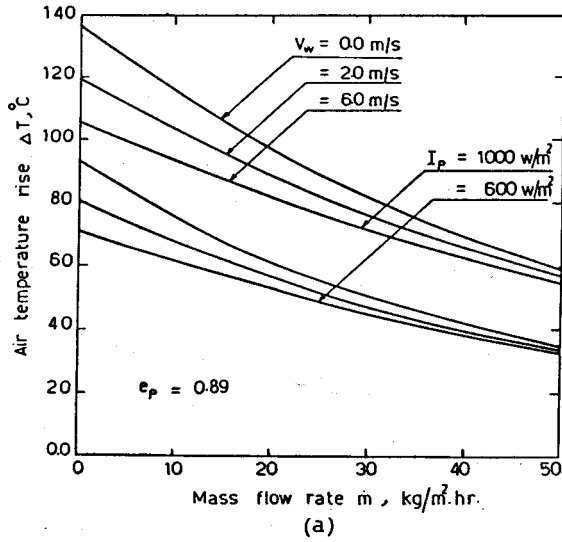


Fig. (4) : Dependence of air temperature rise at the optimum condition on wind speed  $V_w$ , air mass flow rate  $\dot{m}$  for : a)  $e_p = 0.89$  & b)  $e_p = 0.2$ .

Finally in comparing Figure 5 for the effect of system parameters on the collector efficiency, it can be seen that while the air temperature rise decreases by increasing the flow rate, the collector efficiency is improved. Therefore, reaching a high outlet temperature is always accomplished at the expense of low efficiency.

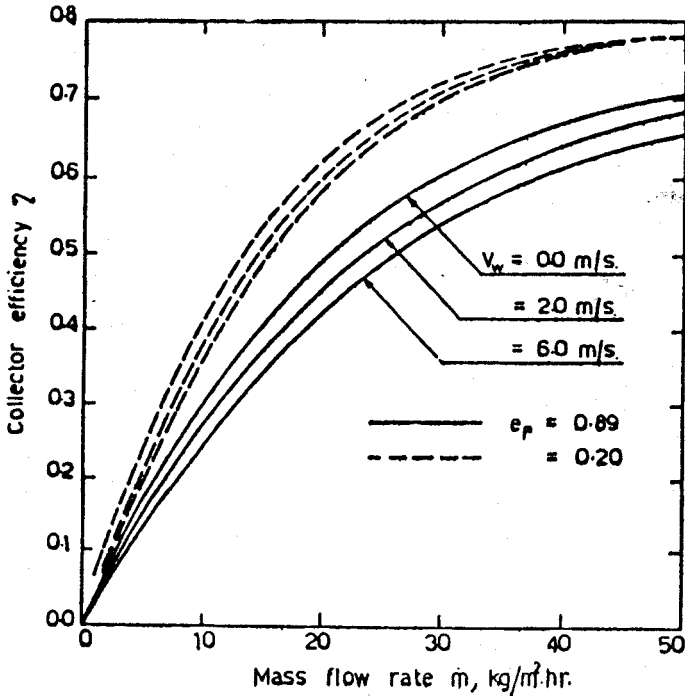


Fig. (5) : Collector efficiency at the optimum condition as a function of air mass flow rate  $\dot{m}$ , and wind speed  $V_w$  for  $I_p = 600 \text{ w/m}^2$  and  $e_p = 0.89$  &  $0.20$ .

To explain the effect of the mass flow rate on the performance of the collector, Figure 6 presents some air temperature profiles at the optimum conditions, ( $Ra_{sys} = Ra_c$ ), for  $I_c = 600 \text{ W/m}^2$  and  $e_p = 0.89$ . As the flow rate is increased, the temperature profile tends to be more flat near the cover surface and more steep near the other side. A further increase in the air flow rate creates a thermal boundary layer with a thickness less than the air layer thickness. Thus, for flow

*An Optimum Performance of a Flat-typed Solar Air Heater*

rates  $m < 40 \text{ Kg/m}^2 \text{ hr}$ , the heat penetrating to the cover is by conduction and radiation while for  $m > 40 \text{ Kg/m}^2 \text{ hr}$ , the heat transfer to the cover is due to radiation only. However, the intensity of radiation exchange between the cover and the absorber is much decreased as the mass flow rate increases. This is shown in Figure 7. This figure also indicates the contribution of radiative and conductive heat exchange between the two surfaces. Radiation transfer is much more important than conduction for  $e_p = 0.89$ . While for  $e_p = 0.2$ , the conduction loss is larger than radiation exchange for  $m < 18 \text{ Kg/m}^2 \text{ hr}$ , and vice versa for  $m$  larger than this value. Lastly, the figure also explains the reason for the variation of the efficiency with the flow rate and the emissivity by a plot of the useful heat gain.

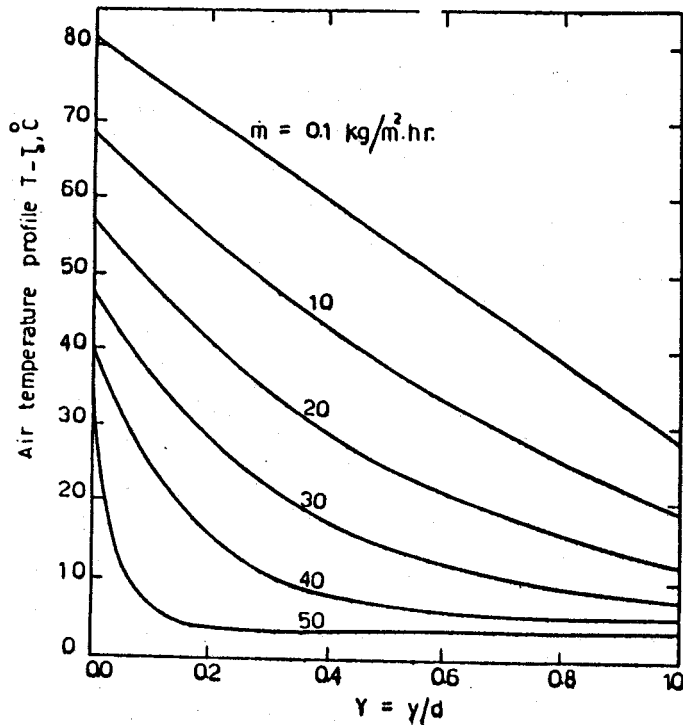


Fig. (6) : Effect of air mass flow rate  $m$  on the air temperature profiles at optimum conditions for  $V_w = 2 \text{ m/s}$  &  $I_p = 600 \text{ w/m}^2$ .



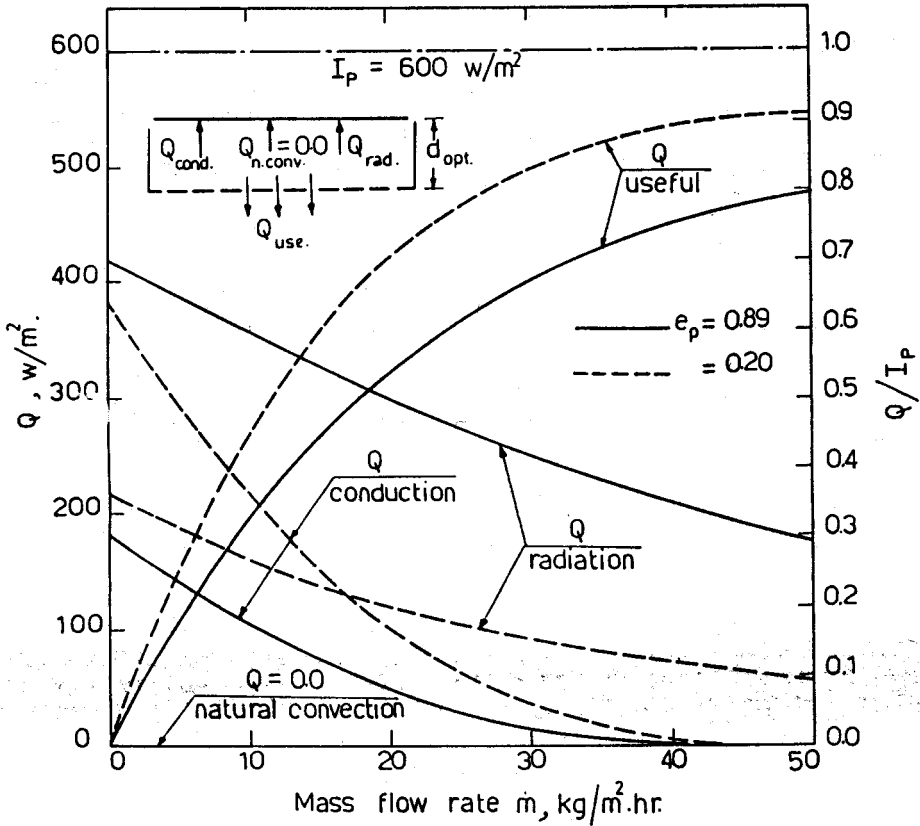


Fig. (7) : Collector energy balance corresponding to the optimum condition for  $V_w = 2 \text{ m/s}$ ,  $I_p = 600 \text{ w/m}^2$  and  $e_p = 0.89$  &  $0.2$ .

## 5. CONCLUSIONS

Conclusions of this investigation can be summarized as follows:

1. In order to determine the optimum efficiency of a flat plate solar air heater, it is necessary first to determine the air layer thickness corresponding to specific operating and environmental conditions.

*An Optimum Performance of a Flat-typed Solar Air Heater*

2. The present model in its simplest form indicates that air can be produced at moderate temperatures (60–80)°C, with efficiencies higher than 60%. With a selective coating absorber, collectors can provide air at elevated temperatures higher than 100°C with an efficiency higher than 60%.

**ACKNOWLEDGEMENT**

This paper is a part of a research project under Grant FRCU No. 82007 between the University of Alexandria, Egypt and the University of Wisconsin at Madison, U.S.A.

**REFERENCES**

1. Hollands, K.G.T.: "Honeycomb Devices in Flat Plate Solar Collectors", Solar Energy, Vol. 9, pp. 159–164, (1965).
2. Charters, W.W.S. and Peterson, L.F.: "Free Convection Suppression Using Honeycomb Collector Materials", Solar Energy, Vol. 13, pp. 353–361, (1972)\*.
3. Buchberg, H., Lalude, O.A. and Edwards, D.K.: "Performance Characteristics of Rectangular and Honeycomb Solar-Thermal Convertors", Solar Energy, Vol. 13, pp. 193–221, (1971).
4. Catton, I.: "Convection in a Closed Rectangular Region: The Onset of Motion", Journal of Heat Transfer, pp. 186–188 (1970).
5. Edwards, D.K.: "Suppression of Cellular Convection by Lateral Walls", Journal of Heat Transfer, pp. 145–150, (1969).
6. Buchberg, H., Catton, I. and Edwards, D.K.: "Natural Convection in Enclosed Spaces – A Review of Application to Solar Energy Collection", Journal of Heat Transfer, pp. 182-188, (1976).
7. Gershuni, G.Z. and Zhukhovitskii, E.M.: "Convective Stability of Incompressible Fluids", Sec. 39, (Ketter Publ. House, 1976).
8. Hassab, M.A.: "Cellular Convection in a Fluid Layer Between Two Porous Plates with Non-uniform Volumetric Heat Sources", Proceedings of the 16th South Eastern Seminar on Thermal Sciences, Miami, U.S.A., 16–18 April, (1982).
9. Elewa, F.: "Effect of Suction on Instability of Fluid in Inclined Solar Collectors", M.Sc. Thesis, Mechanical Engineering Department, Alexandria University, (1983).
10. Kopela, S.A., Gozu, D. and Baxi, C.B.: "On the Stability of the Conduction Regime in a vertical Slot". Int. J. Heat mass Transfer 16, 1983-1960, (1973).